FEBS Letters 362 (1995) 10–14 FEBS 15268

Hypothesis

The active site of the cyanide-resistant oxidase from plant mitochondria contains a binuclear iron center

James N. Siedow[a,*], Ann L. Umbach[a], Anthony L. Moore[b]

[a]*DCMB/Botany, Box 91000, Duke University, Durham, NC 27708-1000, USA*
[b]*Biochemistry Department, University of Sussex, Falmer, Brighton BN1 9QG, UK*

Received 18 January 1995

Abstract The cyanide-resistant, alternative oxidase of plant mitochondria catalyzes the four-electron reduction of oxygen to water, but the nature of the catalytic center associated with this oxidase has yet to be elucidated. We have identified conserved amino acids, including two copies of the iron-binding motif Glu-X-X-His, in the carboxy-terminal hydrophilic domain of the alternative oxidase that suggest the presence of a hydroxo-bridged binuclear iron center, analogous to that found in the enzyme methane monooxygenase. Using the known three-dimensional structures of other binuclear iron proteins, we have developed a structural model for the proposed catalytic site of the alternative oxidase based on these amino acid sequence similarities.

Key words: Cyanide-resistant oxidase; Binuclear iron protein; Plant mitochondria; Active site model

1. Introduction

A major characteristic of plant mitochondria is the presence of a cyanide- and antimycin-resistant 'alternative' oxidase in addition to the conventional cytochrome *c* oxidase [1]. This terminal oxidase branches from the main respiratory chain at the level of the ubiquinone pool, is not energy conserving, reduces O_2 to H_2O and is inhibited by primary benzohydroxamic acids such as salicylhydroxamic acid [1,2].

cDNA clones encoding the alternative oxidase protein have been reported from several plant species, including *Sauromatum guttatum*, *Arabidopsis*, soybean and tobacco [3–6], as well as the yeast *Hansenula anomala* [7]. Hydropathy analysis of the deduced amino acid sequences of all alternative oxidase cDNAs sequenced to date predicts that two regions, located roughly in the center of the protein, are hydrophobic, strongly α-helical and of sufficient length to be membrane spanning [1,3,7]. The remainder of the protein is quite hydrophilic, with charged residues distributed over much of its mass. The current model for the structure of the alternative oxidase protein postulates two large hydrophilic domains, on either side of the two membrane-anchoring helices [1]. This model has both hydrophilic domains located on the matrix side of the inner mitochondrial membrane [8,9].

The ability of the alternative oxidase to reduce oxygen to water suggests that the active site of the oxidase contains a coupled transition metal center, by analogy with other known water-forming oxidases [10]. Previous metal analyses of partially purified alternative oxidase preparations have been inconclusive; Fe, Cu and Mn have each been reported in varying amounts [11–13]. Among the alternative oxidase amino acid sequences, no motifs common to metal binding sites reported for other proteins have been identified to date [1,3,7]. The best evidence that iron is associated with the alternative oxidase active site comes from the results of Minagawa et al. [14] who found that induction of the alternative pathway in *H. anomala* in the presence of antimycin and the Fe(II) chelator *o*-phenanthroline led to the synthesis of the 36 kDa alternative oxidase protein, but no measurable alternative pathway activity. The subsequent addition of Fe(II) to the cells led to the rapid appearance of alternative pathway activity.

Analyses of isolated plant mitochondria using electron paramagnetic resonance (EPR) spectroscopy indicated neither any resonances unique to plant mitochondria nor any whose redox behavior were indicative of a specific association with the alternative pathway [15,16]. A partially purified alternative oxidase preparation from *Symplocarpus foetidus* spadices also showed no EPR resonances in either the oxidized or the dithionite-reduced states and had no optical absorbance above 350 nm [17]. Preliminary analysis of one *S. foetidus* preparation using atomic absorption spectroscopy has indicated the presence of iron (A.L. Umbach, unpublished observation).

The soluble form of the enzyme methane monooxygenase catalyzes the hydroxylation of methane to methanol [18]. The enzyme consists of three subunits in an $\alpha_2\beta_2\gamma_2$ arrangement, with the α subunit containing the catalytic site at which the hydroxylation reaction takes place. Based on physical properties and conserved amino acid sequence motifs, the active site of the hydroxylase subunit contains a bridged binuclear iron center having structural features analogous to other Fe-O-Fe metalloproteins, such as hemerythrin, the R2 subunit of ribonucleotide reductase and soluble eukaryotic fatty acyl desaturases [19–21]. In all of these enzymes, the oxidized protein contains antiferromagnetically coupled high-spin Fe(III) atoms [19,22]. In the fully reduced state, both iron atoms are Fe(II) and remain coupled, although probably ferromagnetically [19]. As a result, these binuclear iron proteins show no standard EPR signal in either the oxidized or fully reduced states. However, fully reduced [Fe(II)Fe(II)] methane monooxygenase does display an integer spin EPR signal at $g = 16$ [23]. Unique to methane monooxygenase among these binuclear iron proteins is the absence of any optical absorbance above 300 nm in the oxidized state [19,22].

*Corresponding address. Fax: (1) (919) 613-8177.
E-mail: jsiedow@acpub.duke.edu

SSDI 0014-5793(95)00196-4

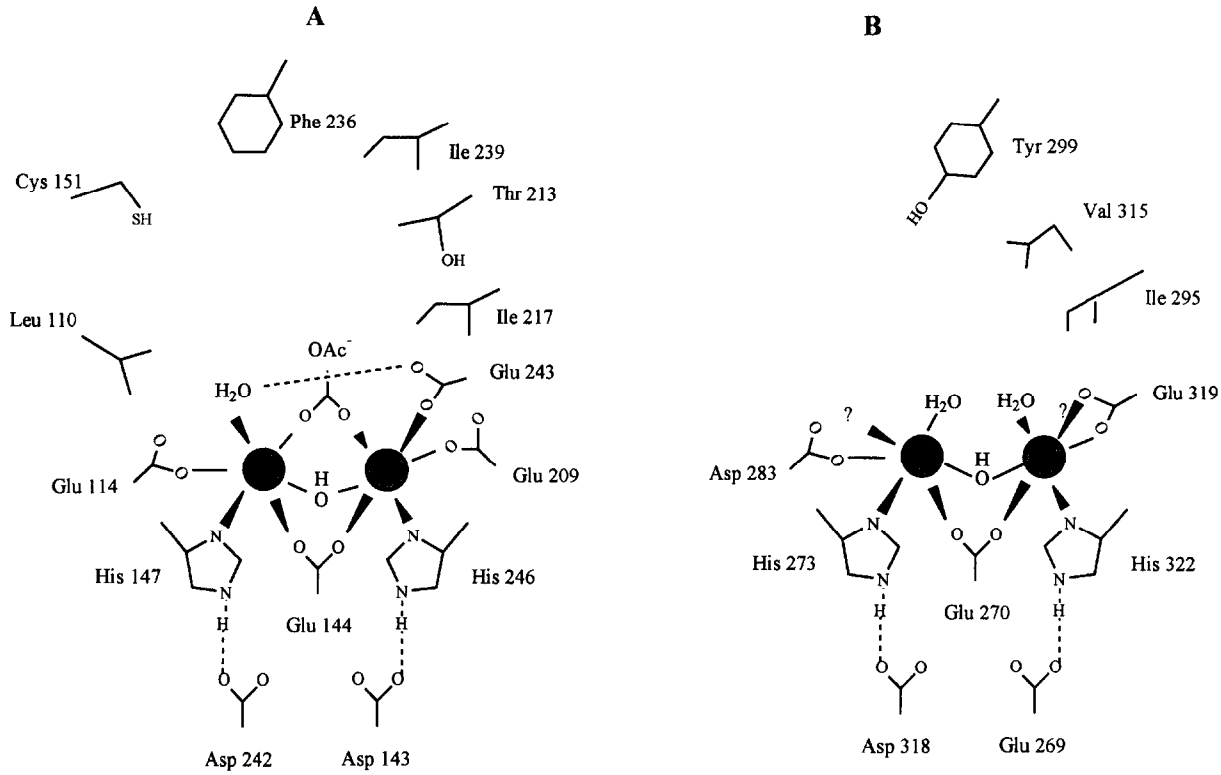

Fig. 1. Diagrammatic representation of the liganding pattern for the coupled binuclear iron center of the *Methylococcus capsulatus* methane monooxygenase and the proposed center of the alternative oxidase. (A) The iron center of methane monooxygenase is coordinated by two histidines, four glutamates, a bridging hydroxide, one water molecule and a bridging acetate [26]. All residues shown are conserved among methane monooxygenases and within a wide range of other binuclear iron proteins [20,21]. (B) In the proposed active site of the cyanide-resistant, alternative oxidase, conserved residues are arranged as outlined in the text to best accommodate the coupled binuclear iron center. The residue numbers refer to the amino acid sequence for the unprocessed polypeptide from *S. guttatum* [3].

The three-dimensional structures of three binuclear iron proteins (hemerythrin, the R2 subunit of ribonucleotide reductase and the α subunit of methane monooxygenase) are currently known [24–26]. The exact liganding side chains vary among the different proteins but in every case, the iron center is buried within a scaffold of four long (30–35 residues) α helices organized in a four-helical bundle. In methane monooxygenase and ribonucleotide reductase, two of the four helices in the bundle each contain the sequence Glu-X-X-His, which is a recurring motif in many oxo-bridged diiron proteins [20–22]. Both of the histidines and one of the two carboxylates serve as monodentate ligands to the iron atoms in the binuclear cluster, while the second carboxylate acts as a bidentate ligand, bridging the two iron atoms (Fig. 1A). The remaining protein ligands to the iron atoms are provided by carboxylate residues, one in each of the other two helices of the four-helical bundle. In methane monooxygenase, the liganding histidines are further stabilized within the structure by hydrogen bonding to the side chain of a conserved carboxylate residue immediately N-terminal to the glutamate residue within each opposing Glu-X-X-His sequence. Methane monooxygenase also differs from the R2 protein of ribonucleotide reductase by having a hydroxo species as the bridging oxygen instead of a μ-oxo group. The absorbance in the 300–400 nm region of ribonucleotide reductase has been assigned to an oxo → Fe^{3+} charge transfer band [27] which is shifted to lower wavelengths when the oxygen is protonated [28], accounting for the lack of electronic absorption above 300 nm in methane monooxygenase. An additional feature of both the methane monooxygenase and ribonucleotide reductase active sites is the presence of a hydrophobic cavity formed adjacent to the iron center by a series of conserved residues within the four-helical bundle (Fig. 1A).

2. Results and discussion

The lack of any standard EPR signals as well as any absorbance above 350 nm by the oxidized and fully reduced forms of methane monooxygenase, unusual properties for a metalloprotein, was reminiscent of the partially purified alternative oxidase [17] and led us to ascertain whether there were any amino acid sequence similarities between these two proteins. Among the four reported plant alternative oxidase sequences [3–6] and an unpublished sequence from potato (L. McIntosh, personal communication), each contains two conserved regions, Glu-Glu-A-I-His and Asp-Glu-A-H-His, in the carboxy-terminal hydrophilic domain of the protein (Fig. 2), beginning just beyond the second membrane-spanning region. These two motifs correspond to those involved in ligating the binuclear iron cluster of methane monooxygenase [26], with the single conservative substitution of a glutamate for an aspartate residue next to the liganding glutamate in the more N-terminal of the two sequences (Fig. 2).

Using this putative iron-binding motif in the alternative oxidase, a model of a binuclear iron center in the protein was developed. The four-helical bundle that forms the metal binding site in the well-characterized binuclear iron proteins contains 30 to 35 residues per helical region [24–26], with two of the four helices each containing one of the two Glu-X-X-His motifs in the R2 protein and methane monooxygenase [25,26]. The total span from the first through the second Glu-X-X-His motif in the alternative oxidase is just under 60 residues, necessitating shorter helical spans than those present in the known binuclear iron proteins.

Using the numbering for the unprocessed *S. guttatum* amino acid sequence [3], and starting at Glu-268, we developed a model containing four successive helices of 10 to 11 residues each (Fig. 2). In this model, the two Glu-X-X-His iron-binding motifs are located on helices 1 and 4, which are oriented antiparallel (Fig. 3), analogous to helices C and F in methane monooxygenase. Helix 2 in this model contains a conserved aspartate residue (Asp-283) located toward the amino terminus which positions it to act as a ligand to iron atom Fe1 (analogous to Glu-114 in Helix B of methane monooxygenase [26]) (Fig. 1A). Missing from this model is a conserved aspartate or glutamate residue in Helix 3 that serves as the analogue to Glu-209

```
                <-----Helix 1----->          <-------Helix 2-------->
G.m.   240  E E E A I H S Y T E F L K E L D K . . . G N I E N
A.t.   224  - - - - - - - - - - - - - - - - . . . - - - - -
N.t.   272  - - - - - - - - - - - - - - - - . . . - - - - -
S.g.   268  - - - - - - - - - - - - D I - S . . . - A - Q D
H.a.   232  - - - - V S T - - H L I - D - - - K R L P K F D D

MMO    142  L D E I R H T H Q C  112  V G E Y N A I A A T G M
R2     113  F S E T I H S R S Y   82  L L D S I Q G R S P N V
Desat  174  A E E N R H G D L L  144  Y Q T M L N T L D G V R

                      <------Helix 3------>
G.m.   262  V P A P A I A I D Y W . Q L P P G S T
A.t.   246  - - - - - - - - - - . R - - A D A -
N.t.   294  - - - - - - - - - - C . R - - K D - -
S.g.   290  C - - - - - - L - - - . R - - Q - - -
H.a.   257  - N L - E - S W L - - T D - N E K - -

MMO    208  G E A C F T N P L I V A V T E W A A A
R2     203  L E A I R F Y V S F A C S F A F A E R
Desat  227  F Q E R A T F I S H G N T A R Q A K E

                            <------Helix 4------>
G.m.   280  L R D V V M V V R A D E A H H R D
A.t.   264  - - - - - - - - - - - - - - - -
N.t.   312  - L - - - L - - - - - - - - - -
S.g.   308  - - - - - T - - - - - - - - - -
H.a.   276  F - - L I Q R I - - - - S K - - E

MMO    232  T P T V F L S I E T D E L R H M A
R2     227  N A K I I R L I A R D E A L H L T
Desat  251  L A Q I C G T I A A D E K R H E T
```

Fig. 2. Comparison of the alternative oxidase deduced amino acid sequences within the region of the proposed binuclear iron center. All alternative oxidase sequences are aligned relative to the conserved glutamate residue (Glu-270) of *S. guttatum* [3]. The sequences represented are for the unprocessed alternative oxidase proteins from soybean (*G.m.*) [5], *Arabidopsis* (*A.t.*) [4], tobacco (*N.t.*) [6], *S. guttatum* (*S.g.*) [3] and *H. anomala* (*H.a.*) [7]. Bold residues represent amino acids that are involved directly in the formation of the coupled binuclear iron center, as outlined in the text. Dashes (−) denote residues identical to those found in the soybean sequence, and dots (.) are used to indicate breaks in the plant amino acid sequences needed to maximize the alignment of conserved residues in the *H. anomala* sequence. Also shown are the amino acid sequences of the iron-binding regions of other binuclear iron proteins: *M. capsulatus* methane monooxygenase (MMO) [20], *E. coli* ribonucleotide reductase R2 protein (R2) [20] and castor bean stearoyl-ACP desaturase (Desat) [21].

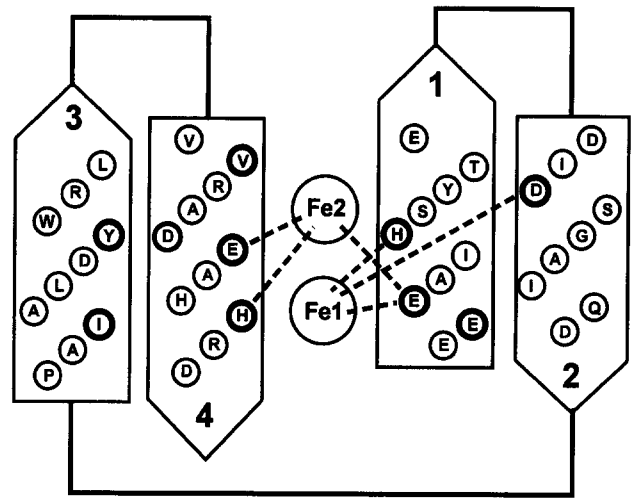

Fig. 3. Diagrammatic representation of the four α-helical bundle that provides the iron-coordinating ligands in the proposed active site of the alternative oxidase. The helices shown contain the amino acids from the *S. guttatum* sequence (Fig. 2) and begin with the most amino terminal of the four proposed helices (Helix 1). The triangular end on each helical stretch is associated with the carboxy terminus of the helix. Helices 1, 2, 3 and 4 of the alternative oxidase correspond to Helices C, B, E and F of methane monooxygenase [20,26], respectively, which conserves the topological orientation of the two iron-binding motifs within the four helical scaffold.

in Helix E of methane monooxygenase and, hence, the final carboxylate ligand to iron atom Fe2 [19]. Interestingly, the soluble fatty acyl desaturases, which clearly contain a binuclear iron center, also lack a conserved carboxylate in Helix B [21]. In addition, in the R2 protein of *E. coli* ribonucleotide reductase, Asp-84 in Helix B, the analogue to Glu-114 in methane monooxygenase, acts as a bidentate ligand to Fe1 [25]. If Glu-319 in Helix 4 were to doubly coordinate iron atom Fe2 in the alternative oxidase active site in a fashion analogous to that of Asp-84 binding to Fe1 in ribonucleotide reductase, the need for the additional carboxylate ligand in Helix 3 would be eliminated. Like methane monooxygenase, the conserved carboxylate residue adjacent to each Glu-X-X-His sequence is positioned to hydrogen bond to the liganding histidine of the alternate Glu-X-X-His (Fig. 1B). Finally, a bridging hydroxo atom is incorporated into the alternative oxidase active site model (Fig. 1B) to account for the lack of absorbance above 300 nm, analogous to methane monooxygenase [19,22].

The four-helical bundle shown in Fig. 3 requires tight turns containing three residues each at the Helices 1/2 and 2/3 junctions. Analogous tight turns have been found previously in proteins having a four helix-bundle motif [24,29]. The alignment of the two Glu-X-X-His iron-binding motifs on Helices 1 and 4 can be arranged exactly as found in methane monooxygenase Helices C and F, respectively [26]. Helix 4 also contains a conserved valine at position 315, three residues to the amino-terminal side of Asp-318. This puts Val-315 in a position analogous to that of Ile-239 in methane monooxygenase (Fig. 1), a residue that lines the hydrophobic pocket in the active site [26] and is conserved as either an isoleucine or a valine among all methane monooxygenases, ribonucleotide reductases and the soluble fatty acyl desaturases (Fig. 2) [20,21]. In Helix 3 of the proposed alternative oxidase active site, the conserved residue,

Tyr-299, can be aligned within the hydrophobic pocket in the position occupied by Ile-217 and Phe-212 in Helix E of methane monooxygenase and the R2 protein of ribonucleotide reductase, respectively (Figs. 2 and 3). In ribonucleotide reductase, Phe-212 combines with Phe-208 (equivalent to Thr-213 in methane monooxygenase) to line the hydrophobic pocket. In the alternative oxidase, Ile-295 in Helix 3 occupies the position analogous to Phe-208 of ribonucleotide reductase and is conserved among all sequences. To summarize, using conserved residues within the plant alternative oxidase amino acid sequence, a structural model incorporating a hydroxo-bridged binuclear iron center held within a four-helix bundle, analogous to the iron center in methane monooxygenase, can readily be developed (Fig. 1B).

When the amino acid sequence reported for the yeast *H. anomala* [7] is adapted to the model shown in Fig. 1B, the degree of residue conservation within the proposed active site between the yeast and the plant sequences is striking (Fig. 2). Neglecting the conservative substitution of an isoleucine for Val-315 in the hydrophobic pocket, the only modification is the lack of a histidine in the Glu-X-X-His motif in Helix 1; this residue is a serine in *Hansenula* (Fig. 2).

While serine could substitute for histidine as a ligand to Fe1 in the active site, this is not an insignificant change, and it could modify the physical properties of the *Hansenula* active site, relative to that of the oxidase from plants. However, other possibilities exist. A unique histidine occurs at position 241 in the *Hansenula* sequence, at the carboxy-terminal end of Helix 1 (Fig. 3). His-241 would be located on the same face of Helix 1 as the other Fe1 ligands, but displaced laterally roughly 3.5 Å and vertically along the helical axis about 6.0 Å from the position of the liganding His-273 in *S. guttatum*. His-241 could be in a position to substitute for the missing histidine residue of the Helix 1 Glu-X-X-His motif in *Hansenula*. There is some precedent for this sort of substitution. Mutation of a cysteine ligand (Cys-20) in the 4Fe-4S cluster of *Azotobacter vinelandii* ferredoxin I to alanine resulted in a structural change that allowed another cysteine, Cys-24, to supply the missing ligand to the cluster [30]. On the other hand, the binuclear iron center in hemerythrin differs from those found in methane monooxygenase and ribonucleotide reductase by the substitution of three liganding carboxylate residues in the latter two proteins with three histidines in hemerythrin. In spite of these marked differences in ligands, which undoubtedly contribute to the functional difference between the oxygen-binding hemerythrin and the two oxygen-activating enzymes, many of the physical properties between the two types of proteins are remarkably similar [21,22].

Although no salicylhydroxamate-sensitive, cyanide-resistant oxidase activity, analogous to the plant oxidase, has been reported in any prokaryotic organism, Kumar and Söll [4] were able to rescue a cytochrome *c* oxidase-deficient mutant strain of *E. coli* by expressing a plasmid-borne cDNA for the *Arabidopsis* alternative oxidase in the bacterium. If the active site of the alternative oxidase contains a binuclear iron center, it could be assembled in the prokaryotic *E. coli* because the latter organism has the metabolic machinery needed to synthesize the binuclear iron center of ribonucleotide reductase.

The presence of a single binuclear iron center in the active site of the alternative oxidase leads to an obvious complication vis-à-vis the four-electron reduction of molecular oxygen to water. There is only enough capacity to accommodate two electrons within the center between the fully oxidized and fully reduced states. Steady-state kinetic analysis suggests that the oxidase reacts with two molecules of reduced ubiquinone before binding and subsequently reducing molecular oxygen [31,32]. An additional two-electron center in the oxidase seems unlikely, given the lack of distinct spectroscopic signatures. One possibility is that the four-electron reduced oxidase suggested by the steady-state kinetic data actually represents the two-electron reduced enzyme plus a bound molecule of reduced ubiquinone. Clearly additional studies are needed to ascertain whether the model presented here can account fully for the catalytic activity of the alternative oxidase.

Acknowledgements: This work was supported by grants from the National Science Foundation (MCB-9407759) to J.N.S. and from the BBSRC to A.L.M. The authors also thank Dr. D.M. Rhoads for his help in producing Fig. 3.

References

[1] Moore, A.L. and Siedow, J.N. (1991) Biochim. Biophys. Acta 1059, 121–140.
[2] Siedow, J.N. and Berthold, D.A. (1986) Physiol. Plant. 66, 569–573.
[3] Rhoads, D.M. and L. McIntosh (1991) Proc. Natl. Acad. Sci USA88, 2122–2126.
[4] Kumar, A.M. and Söll, D. (1992) Proc. Natl. Acad. Sci. USA 89, 10842–10846.
[5] Whelan, J., McIntosh, L. and Day, D.A. (1993) Plant Physiol. 103, 1481.
[6] Vanlerberghe, G.C. and McIntosh, L. (1994) Plant Physiol. 105, 867–874.
[7] Sakajo, S., Minagawa, N., Komiyama, T. and Yoshimoto, A. (1991) Biochim. Biophys. Acta 1090, 102–108.
[8] Rasmusson, A.G., Møller, I.M. and Palmer, J.M. (1990) FEBS Lett. 259, 311–314.
[9] Siedow, J.N., Whelan, J., Kearns, A., Wiskich, J.T. and Day, D.A. (1992) in: Molecular, Biochemical and Physiological Aspects of Plant Respiration (Lambers, H. and van der Plas, L.H.W., Eds.) pp. 19–27, SPB Academic Publishing, The Hague.
[10] Naqui, A. and Chance, B. (1986) Annu. Rev. Biochem. 55, 137–166.
[11] Huq, S. and Palmer, J.M. (1978) FEBS Lett. 95, 217–220.
[12] Palmer, J.M. and Huq, S. (1981) in: Cyanide in Biology (Vennesland, B., Conn, E.E., Knowles, C.J., Westley, J. and Wissing, F., Eds.) pp. 451–460, Academic Press, New York.
[13] Bonner, W.D., Clarke, S.D. and Rich, P.R. (1986) Plant Physiol. 80, 838–842.
[14] Minagawa, N., Sakajo, S., Komiyama, T. and Yoshimoto, A. (1990) FEBS Lett. 267, 114–116.
[15] Rich, P.R., Moore, A.L., Ingledew, W.J. and Bonner, W.D. (1977) Biochim. Biophys. Acta 462, 501–514.
[16] Siedow, J.N. (1982) in: Recent Advances in Phytochemistry (Creasy, L.L. and Hrazdina, G., Eds.) vol. 16, pp. 47–83, Plenum Press, New York.
[17] Berthold, D.A. and Siedow, J.N. (1993) Plant Physiol. 101, 113–119.
[18] Lipscomb, J.D. (1994) Annu. Rev. Microbiol. 48, 371–399.
[19] Wilkins, R.G. (1992) Chem. Soc. Rev. 21, 171–178.
[20] Nordlund, P., Dalton, H. and Eklund, H. (1992) FEBS Lett. 307, 257–262.
[21] Fox, B.G., Shanklin, J., Ai, J., Loehr, T.M. and Sanders-Loehr, J. (1994) Biochemistry 33, 12776–12786.
[22] Vincent, J.B., Olivier-Lilley, G.L. and Averill, B.A. (1990) Chem. Rev. 90, 1447–1467.
[23] Hendrich, M.P., Münck, E., Fox, B.G. and Lipscomb, J.D. (1990) J. Am. Chem. Soc. 112, 5861–5865.
[24] Sheriff, S., Hendrickson, W.A. and Smith, J.L. (1987) J. Mol. Biol. 197, 273–296.

[25] Nordlund, P., Sjöberg, B.-M. and Eklund, H. (1990) Nature 345, 593–598.
[26] Rosenzweig, A.C., Frederick, C.A., Lippard, S.J. and Nordlund, P. (1993) Nature 366, 537–543.
[27] Sanders-Loehr, J., Wheeler, W.D., Shiemke, A.K., Averill, B.A. and Loehr, T.M. (1989) J. Am. Chem. Soc. 111, 8084–8093.
[28] Turowski, P.N., Armstrong, W.H., Liu, S., Brown, S.N. and Lippard, S.J. (1994) Inorg. Chem. 33, 636–645.
[29] Lederer, F., Glatigny, A., Bethge, P.H., Bellamy, H.D. and Mathews, F.S. (1981) J. Mol. Biol. 148, 427–448.
[30] Martín, A.E., Burgess, B.K., Stout, C.D., Cash, V.L., Dean, D.R., Jensen, G.M. and Stephens, P.J. (1990) Proc. Natl. Acad. Sci. USA 87, 598–602.
[31] Siedow, J.N. and Moore, A.L. (1993) Biochim. Biophys. Acta 1142, 165–174.
[32] Ribas-Carbo, M., Berry, J.A., Azcon-Bieto, J. and Siedow, J.N. (1994) Biochim. Biophys. Acta 1188, 205–212.